
Instance Data Condensation for Image Super-Resolution

Tianhao Peng[†], Ho Man Kwan[†], Yuxuan Jiang[†], Ge Gao[†], Fan Zhang[†]
Xiaozhong Xu[‡], Shan Liu[‡], David Bull[†]

[†] Visual Information Lab, University of Bristol, UK

[‡] Tencent Media Lab, Palo Alto, USA.

{tianhao.peng, hm.kwan, yuxuan.jiang, ge1.gao, fan.zhang, dave.bull}@bristol.ac.uk,
{xiaozhongxu, shanl}@tencent.com

Abstract

Deep learning based image Super-Resolution (ISR) relies on large training datasets to optimize model generalization; this requires substantial computational and storage resources during training. While dataset condensation has shown potential in improving data efficiency and privacy for high-level computer vision tasks, it has not yet been fully exploited for ISR. In this paper, we propose a novel Instance Data Condensation (IDC) framework specifically for ISR, which achieves instance-level data condensation through Random Local Fourier Feature Extraction and Multi-level Feature Distribution Matching. This aims to optimize feature distributions at both global and local levels and obtain high-quality synthesized training content with fine detail. This framework has been utilized to condense the most commonly used training dataset for ISR, DIV2K, with a 10% condensation rate. The resulting synthetic dataset offers comparable or (in certain cases) even better performance compared to the original full dataset and excellent training stability when used to train various popular ISR models. To the best of our knowledge, this is the first time that a condensed/synthetic dataset (with a 10% data volume) has demonstrated such performance. The source code and the synthetic dataset have been made available at <https://github.com/>.

1 Introduction

Image super-resolution (ISR) is a well-established research area in low-level computer vision, which aims to up-sample a low-resolution image to higher resolutions, while recovering fine spatial details. In recent years, deep learning inspired methods [29, 51, 21, 28, 40] have been dominant in this field, offering significant improvements over conventional ISR methods based on classic signal processing theory. These learning-based solutions are typically optimized offline with a large training dataset and deployed online for processing arbitrary input images. The training data is thus crucial for maintaining the model generalization ability and for avoiding overfitting issues.

To this end, it is common practice to simply increase the amount of training material, but this introduces two primary issues. (i) Training efficiency: a large amount of training content inevitably leads to higher training costs with longer training time and greater storage/memory requirements [38, 16]. Although efforts have been made to accelerate the training process by using large batch sizes, these cannot fully reduce training costs due to increased memory consumption [30]. (ii) Data quality: increased data volume does not guarantee performance improvement - large datasets can be associated with unbalanced content distributions (or bias) and data redundancy, which may result in suboptimal inference performance on certain content and reduced model generalization [62]. Moreover, privacy concerns can also arise when using large-scale data, as models can inadvertently memorize sensitive

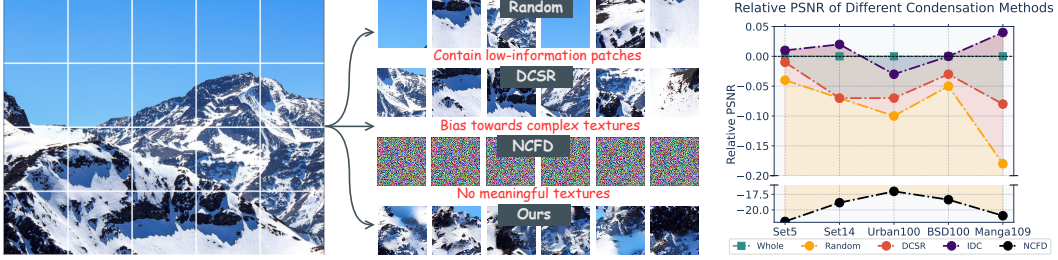


Figure 1: **(Left)**: Visual comparison between synthetic patches generated by our IDC framework and those selected/synthesized by Random Selection, DCSR [9], and NCFD (v1 in our ablation study) [46]. IDC’s patches contain more diverse information than selection-based methods, and data condensation techniques like NCFD (designed for high-level vision) fail to produce meaningful results. **(Right)**: Quantitative results show that an IDC-synthesized dataset (10% volume) can outperform the full DIV2K dataset when training ISR models.

information, making them vulnerable to membership inference attacks that could potentially expose training data details [32, 35].

To address these problems, various dataset refinement approaches have been proposed, including coresets selection [52, 39, 23] and dataset pruning [9, 36], which result in a smaller, representative subset, derived from the large training dataset based on gradient or deep feature statistics. However, these content selection/pruning methods are constrained by the characteristics of the original content, and hence they cannot achieve optimal performance compared to the large dataset, in particular when the subset is much smaller than the original. It is also noted that dataset distillation [47] and condensation [62, 61, 46, 42] techniques have been proposed recently for high-level computer vision tasks (e.g., image classification with ground truth labels). These are designed to distill/condense a large dataset into a small but “informative” version with *synthetic* content. The aim is to achieve improved training efficiency, comparable model generalization ability (with the original dataset), and enhanced data privacy [4, 11]. However, these techniques cannot be directly applied to low-level tasks, such as ISR, due to the requirement for image labels. Although there have been early attempts that focus on ISR dataset condensation [59, 8], these exhibit relatively poor performance or can only be deployed for limited application scenarios.

In this context, this paper proposes a new **Instance Data Condensation (IDC)** framework specifically for image super-resolution, which can significantly reduce the amount of training material and speed up the training process, while maintaining (or even enhancing) the model performance. Taking all the cropped patches from each individual image (instance) in a large dataset as input, this framework generates a small amount of synthetic low-resolution training patches with *condensed* information based on **Random Local Fourier Features** and **Multi-level Feature Distribution Matching**. These methods are designed to retain the distribution of the local features in the original patches and ensure the fidelity and diversity of the synthesized patches. These synthetic low-resolution patches are then up-sampled by a pre-trained ISR model to obtain their high-resolution counterparts. Targeting ISR, this framework has been utilized to condense the most commonly used training dataset in the ISR literature, DIV2K [1], resulting in a synthetic dataset with only 10% training patches. The condensed dataset was then used to train three popular ISR network architectures, EDSR [29], SwinIR [28] and MambaIRv2 [17], which achieve similar or even better evaluation performance compared to the same networks trained with the full DIV2K dataset.

The main contributions of this work are summarized below.

1. We propose a new data condensation framework specifically for ISR that operates at the **instance (image) level**, which addresses the issues when condensing unlabeled datasets. It is the **first time** that a highly condensed dataset has achieved better performance than the original full dataset when used for training ISR models (as shown in Figure 1.(Right)).
2. We designed a **Multi-level Feature Distribution Matching** approach, which learns the feature distribution at both instance and group levels, enhancing the learned feature quality and diversity. Synthesized images by IDC are well-conditioned, enabling high-quality visual feature learning in distribution matching, as shown in Figure 1.(Left).

3. We developed the novel **Random Local Fourier Features**, which captures high-frequency details and local features to facilitate distribution matching in learning high-fidelity synthetic images.

2 Related Work

Image Super-Resolution (ISR) is a fundamental task in low-level computer vision that aims to reconstruct high-resolution (HR) images from their low-resolution (LR) counterparts. Over the past decade, advances in deep learning have significantly improved super-resolution performance, employing ISR models based on network architectures including convolutional neural networks (CNNs) [10, 24, 29, 60], vision transformers [27, 51, 28, 22, 64, 5], and structured state-space models [18, 40, 43, 17]. These ISR methods, due to their data-driven nature, are typically trained offline on a large training dataset and then deployed online for real-world applications. In this case, the training dataset is critical to model performance and generalization.

To facilitate ISR model training, a series of datasets have been developed including small ones such as T91 [53] and BSD200 [34], which contain 91 and 200 natural images, respectively. A significant milestone was the release of DIV2K [1], consisting of 800 high-resolution images, which is now the most commonly used training dataset for ISR. Other alternatives also exist including Flickr2K [44] that comprises 2,650 high-resolution images collected from online sources, LSDIR [26] with more than 85,000 images, and HQ-50K [54] containing 50,000 high-quality images. In this paper, we solely employ DIV2K as the original training dataset to demonstrate the data condensation process due to its popularity. Based on the common practice in ISR literature [48], existing methods typically crop each image in the training dataset into small patches. For example, the 800 original images in DIV2K [1] along with their corresponding low-resolution counterparts (e.g., down-sampled by a factor of 4) are partitioned into overlapped patches, producing approximately 120K pairs (LR and HR), which are used in the training process as the input (LR) and output target (HR) of ISR models.

Dataset condensation and distillation aims to condense or distill a large-scale original training set into a smaller synthetic one, capable of offering comparable performance on unseen test data when used to train a model for a downstream task. Based on the optimization objectives, current dataset condensation methods can be categorized into three classes: performance matching, parameter matching, and distribution matching. *Performance matching* based approaches [47, 65] are designed to optimize the synthetic dataset to achieve minimum training loss (for the downstream task) compared to using the original training dataset, while *parameter matching* [62, 3, 6, 13, 57] encourages models trained on the synthetic dataset to maintain consistency in the parameter space with those trained on the original dataset. Both types of approaches are similar to bi-level meta-learning [14] and gradient-based hyperparameter optimization techniques [62, 13, 57, 33], which are associated with high computation graph storage costs and are difficult to apply to high resolution and large scale datasets [62, 3, 56]. *Distribution matching* generates synthetic data by directly optimizing the distribution distance between synthetic and real data, which typically leverages feature embeddings extracted from networks with different initializations to construct the distribution space, utilizing Maximum Mean Discrepancy (MMD) as the distribution metric [61, 45, 63]. This has been further enhanced by incorporating batch normalization statistics [55, 12, 42] or neural features in the complex plane [46], to achieve enhanced performance on large-scale datasets.

For ISR, multiple contributions have targeted the generation of a small subset of representative samples, based on diversity criteria such as texture complexity and blockiness distributions [9, 36, 37]. Given the distinct differences between image classification and ISR, it is difficult to directly apply the dataset distillation/condensation techniques mentioned above to the ISR task [31]. To the best of our knowledge, there has been very limited investigation into this research topic, with only one notable work [59], which utilizes GAN-based pretrained models to generate synthetic training images. However, This is still only applicable on an SR dataset with labels [49].

3 Method

3.1 Preliminaries

Data condensation for ISR. The training of ISR models employs paired high- and low-resolution (HR and LR) image patches, typically with a spatial resolution larger than 192×192 (for HR patches) [29, 60, 28, 17, 48]. However, most current mainstream dataset condensation methods proposed for

high-level vision tasks are designed and validated on much lower resolution content (e.g. 32×32 or 64×64) [47, 62, 61, 46, 42]. As a result, there are significant challenges when these methods are directly applied to the ISR task. First, the training with high-resolution images that contain more pixels requires significantly increased optimization space (e.g., memory, gradients, etc.), resulting in a much slower (or even impossible) training process. This is in particular relevant to the dataset condensation methods based on performance or gradient matching. Secondly, existing data condensation methods often rely on class labels to calculate task losses (such as the cross-entropy loss, soft labels, etc.) to guide the optimization of synthetic samples, while commonly used datasets in ISR tasks (e.g., DIV2K [1]) are not associated with real class labels.

In this paper, our approach is based on distribution matching, which minimizes the distance of distributions between two datasets. Specifically, given a real, original dataset \mathcal{T} to a synthetic dataset \mathcal{S} , $|\mathcal{S}| \ll |\mathcal{T}|$. The optimization goal is formulated as:

$$\mathcal{S} = \underset{\mathcal{S}}{\operatorname{argmin}} \mathcal{L}(\mathcal{S}, \mathcal{T}), \quad (1)$$

where \mathcal{L} stands for the distance measurement function.

Distance measurement functions. Early approaches [61, 45, 63] employ Mean Squared Error (MSE) or Maximum Mean Discrepancy (MMD) as \mathcal{L} , while recently, Neural Characteristic Function Discrepancy (NCFD) [46] has been proposed to capture distributional discrepancies by aligning the phases and amplitudes of neural features in the complex plane, achieving a balance between realism and diversity in the synthetic samples. Specifically, the optimization process is described by:

$$\min_{D_S} \max_{\psi} \mathcal{L}_{dist}(D_{\mathcal{T}}, D_S, f, \psi) = \min_{D_S} \max_{\psi} \mathbb{E}_{\mathbf{x} \sim D_{\mathcal{T}}, \hat{\mathbf{x}} \sim D_S} \int_t \sqrt{\operatorname{Chf}(\mathbf{t}; f)} dF(\mathbf{t}; \psi), \quad (2)$$

in which

$$\begin{aligned} \operatorname{Chf}(\mathbf{t}; f) = & \underbrace{\alpha \left(\left(|\Phi_{f(\mathbf{x})}(\mathbf{t}) - \Phi_{f(\hat{\mathbf{x}})}(\mathbf{t})| \right)^2 \right)}_{\text{amplitude difference}} \\ & + \underbrace{(1 - \alpha) \cdot (2 |\Phi_{f(\mathbf{x})}(\mathbf{t})| |\Phi_{f(\hat{\mathbf{x}})}(\mathbf{t})| \cdot (1 - \cos(\mathbf{a}_{f(\mathbf{x})}(\mathbf{t}) - \mathbf{a}_{f(\hat{\mathbf{x}})}(\mathbf{t}))))}_{\text{phase difference}}. \end{aligned} \quad (3)$$

Here D denotes the distribution of a dataset. f is the feature extractor that maps input training samples, i.e., $\mathbf{x} \in \mathcal{T}$ or $\hat{\mathbf{x}} \in \mathcal{S}$, into the latent space. $F(\mathbf{t}, \psi)$ is the cumulative distribution function of the frequency argument \mathbf{t} , while ψ is a parameterized sampling network to obtain the distribution of \mathbf{t} . $\Phi_{f(\mathbf{x})}(\mathbf{t}) = \mathbb{E}_{f(\mathbf{x})} [e^{j\langle \mathbf{t}, f(\mathbf{x}) \rangle}]$ stands for the characteristic function. $\operatorname{Chf}(\mathbf{t}; f)$ calculates the distributional discrepancy between training and synthesized samples in the complex plane - here *phase* stands for data centers which is crucial for realism, and *amplitude* captures the distribution scale, contributing to the diversity. α is a hyper-parameter to balance the amplitude and phase information during the optimization process.

It is noted that while NCFD [46] has contributed to the SOTA dataset condensation method for image classification, it cannot capture sufficient high-frequency details and rich local semantic information when directly applied to condense training datasets for ISR. This is illustrated in Figure 1. This may be because it uses a random Gaussian matrix for mapping features - $f(\cdot)^{N \times C \times H \times W} \mapsto f(\cdot)^{N \times D}$ (when the sampling network is not used [46]) - (i) the random Gaussian projection fuses information globally while preserving the spatial structure of the feature maps, which, however, is unsuitable for many low-level vision tasks including ISR, where the fine-grained local information, such as textures, is more important than the high-level structure like shapes; (ii) it does not capture the high-frequency features within high-resolution feature maps extracted by ISR models, thus limiting the capacity to learn fine details in the synthesis process.

3.2 Instance Data Condensation

To address the above issues, specifically for the ISR task, we propose a novel **Instance Data Condensation** (IDC) framework, which performs distribution matching for the local features at multiple levels. This approach efficiently handles the requirements of high-resolution patches for training ISR models and effectively preserves high-frequency details in the original dataset. The proposed IDC framework, shown in Figure 2, generates synthetic training patch pairs in two stages.

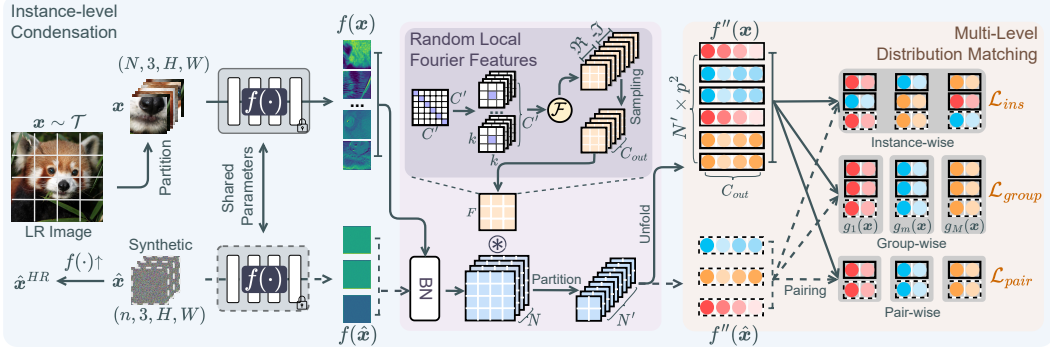


Figure 2: Illustration of the proposed Instance Data Condensation (IDC) framework.

In the first stage, given a real training dataset \mathcal{T} , which contains training patch pairs cropped from C original, high-resolution (HR) images and their low-resolution counterparts, we first perform teacher ISR model training, which will be used in the distribution matching process. We then consider each image as an individual class, and take its corresponding, LR training patches $x \in \mathbb{R}^{N \times 3 \times H \times W}$ as the input of the distribution matching process. A set of synthetic patches $\hat{x} \in \mathbb{R}^{n \times 3 \times H \times W}$ will then be registered as learnable parameters, which are eventually the LR output synthetic patches of the IDC framework. To reduce computational cost, we utilize the feature extractor f in the teacher ISR model to map x and \hat{x} into the latent space, resulting in $f(x)$ and $f(\hat{x})$, similar to previous works in distribution matching [61, 63, 7, 25, 46]. Here N is the total number of patches cropped from the current RGB image/class. $H \times W$ represents the spatial resolution of the training patches. $r \in (0, 1)$ is the condensation ratio, i.e. $n = N * r$.

As mentioned in Subsection 3.1, the latest distribution matching method [46] employs a random Gaussian matrix for feature matching, which works well when representing the feature distributions of image classification tasks, but cannot capture local high-frequency details that are essential for ISR. In this work, we propose to use **Random Local Fourier Features**, which can represent more fine-grained local features, and unfold the obtained feature maps into a batch of features for performing distribution matching. This enables the capturing of fine local details. As shown in Figure 2, both the real and synthetic feature maps, $f(x)$ and $f(\hat{x})$, are processed to obtain their corresponding local features, $f'(x)$ and $f'(\hat{x})$. Given the extracted local features, we then optimize a **multi-level feature distribution loss**, consisting of an instance-level feature distribution loss \mathcal{L}_{ins} , a group-level feature distribution loss \mathcal{L}_{group} , and a pair-wise loss \mathcal{L}_{pair} , in order to obtain the synthetic LR patches \hat{x} for this image/class.

In the second stage, we employ the pre-trained teacher ISR model to up-sample \hat{x} to obtain their corresponding HR patches \hat{x}^{HR} , which effectively leverages knowledge distillation [19] by directly exploiting the LR-to-HR mapping of the teacher model.

3.3 Random Local Fourier Features

Given that the extracted feature maps of the real training patches are denoted as $f(x) \in \mathbb{R}^{N \times c \times h \times w}$, in which c, h, w are the channel number, size of the feature map, respectively, we first define an identity matrix $I_{C' \times C'}$ and reshape it to a convolutional filter, $E \in \mathbb{R}^{C' \times c \times k \times k}$ where $C' = c \times k^2$, and k is the kernel size. This filter is used to map $f(x)$ from the channel-spatial domain to the channel domain to extract local maps, while keeping the spatial information. To extract the high frequency details, we further apply the Fourier transform \mathcal{F} after extracting local features by E , which in practice, is achieved by directly applying \mathcal{F} to the convolutional filter E in the output channel dimension, and decomposing the real and imaginary parts to form a new Fourier-based convolution filter $F \in \mathbb{R}^{2C' \times c \times k \times k}$:

$$F = [\Re(\mathcal{F}(E)), -\Im(\mathcal{F}(E))]. \quad (4)$$

The feature maps, $f(x)$, are transformed by F , to a more informative representation, $f'(x)$, which fully encodes the local spatial and channel information in the frequency domain that is particularly suitable for data and textures with periodic structures.

Algorithm 1: Instance Data Condensation.

Input: Training dataset $\mathcal{T} = \{\mathbf{x}_c, \mathbf{x}_c^{HR}\}, c = 1, \dots, C$; Synthetic dataset $\mathcal{S} = \emptyset$; ISR model f pre-trained on \mathcal{T} ; image/class index c ; condense ratio r ; instance-level distribution loss weight w_{ins} ; group-level distribution loss weight w_{group} ; pair-wise loss weight w_{pair} ; learning rate η .

for each real patches \mathbf{x}_c in \mathcal{T} **do**

 Randomly initialize the synthetic patches $\hat{\mathbf{x}}_c$, subject to $|\hat{\mathbf{x}}_c| = r|\mathbf{x}_c|$;

 Extract the feature maps using f for \mathbf{x}_c ;

for i in num_iters **do**

 Extract the feature maps using f for $\hat{\mathbf{x}}_c$; ▷ Subsection 3.3

 Extract their Random Local Fourier features and Unfold the feature maps into local patches ;

if i in *warm up* **then**

 Compute $\mathcal{L} = w_{ins}\mathcal{L}_{ins}$;

else ▷ Subsection 3.4

if i in *assigning* **then**

 Increase *grouping*;

 Increase *pairing*;

 Compute $\mathcal{L} = w_{ins}\mathcal{L}_{ins} + w_{group}\mathcal{L}_{group} + w_{pair}\mathcal{L}_{pair}$;

 Update $\hat{\mathbf{x}}_c \leftarrow \hat{\mathbf{x}}_c - \eta \nabla_{\hat{\mathbf{x}}_c} \mathcal{L}$;

$\hat{\mathbf{x}}_c^{HR} = f(\hat{\mathbf{x}}_c) \uparrow$;

$\mathcal{S} = \mathcal{S} \cup \{\{\hat{\mathbf{x}}_c, \hat{\mathbf{x}}_c^{HR}\}\}$;

Output: \mathcal{S}

$$f'(\mathbf{x}) = f(\mathbf{x}) \otimes F. \quad (5)$$

Here, to reduce the size of $f'(\mathbf{x})$ and the complexity for loss computation, we implement channel-wise random sampling to get $F \in \mathbb{R}^{C_{out} \times c \times k \times k}, C_{out} < C'$, and apply batch normalization to $f(\mathbf{x})$ before convolution.

Finally, we partition $f'(\mathbf{x})$ to obtain local feature patches $f''(\mathbf{x}) \in \mathbb{R}^{N' \times C_{out} \times p \times p}$, where $N' = N * \lceil h/p \rceil * \lceil w/p \rceil$, and p is the patch size. In order to learn local features in the later multi-level distribution matching, we further *unfold* $f''(\mathbf{x})$ from $\mathbb{R}^{N' \times C_{out} \times p \times p}$ to $\mathbb{R}^{(N' \times p \times p) \times C_{out}}$, which treats features in the patches as different samples in a batch.

This operation (Random Local Fourier Features) has also been applied to the feature maps of the synthetic patches, $f(\hat{\mathbf{x}})$, before performing the multi-level distribution matching detailed below.

3.4 Multi-level distribution matching

To adapt to the nature of the ISR task, rather than directly using existing distribution matching losses, we propose a Multi-level Distribution Matching approach to optimize the feature distribution of synthetic patches at both instance (class) and group levels and match pair-wise feature patches.

Matching instance-level feature distributions. After obtaining local features for both real and synthetic patches, $f''(\mathbf{x})$ and $f''(\hat{\mathbf{x}})$, the instance-level feature distribution loss, \mathcal{L}_{ins} , is calculated to minimize the distributional discrepancy between the real and synthetic patches, based on NCFD [46]. Here we do not use the sampling network mentioned in its original literature for efficient computation:

$$\mathcal{L}_{ins} = \mathcal{L}_{dist}(\mathbf{x}, \hat{\mathbf{x}}, f) = \mathbb{E}_{\mathbf{x}, \hat{\mathbf{x}}} \int_t \sqrt{\text{Chf}(\mathbf{t}; f)} dF(\mathbf{t}). \quad (6)$$

Matching group-wise feature distributions. While instance-level feature distribution matching ensures consistency in the overall (global) feature distribution between synthetic and original patches, local features often exhibit significant complexity and diversity, preventing instance-level matching from sufficiently capturing all distributional differences. To address this issue, we designed a more fine-grained, group-level feature distribution matching loss, \mathcal{L}_{group} , which first partitions the real local features $f''(\mathbf{x})$ into M groups using K-means algorithm. Each synthetic local feature is then iteratively assigned to its nearest group centroid with a progressive assigning strategy.

Here, the number of synthetic features assigned to each group is proportional to the number of real features in that group, and the assignment is updated in steps to maintain stable optimization. To ensure that the assignments of neighboring features are consistent and to reduce the complexity, the unfolded local features which originally come from the same local feature patch, are grouped together. The resulting grouped local features are denoted as $\{g_m(\mathbf{x})\}$ and $\{g_m(\hat{\mathbf{x}})\}$, $m = 1, \dots, M$.

After this assignment, we compute the feature distribution matching loss for each group to more accurately learn the synthetic data, by reflecting the real data distribution at the group level. This is described by the following equation:

$$\mathcal{L}_{group} = \sum_{m=1}^M \mathcal{L}_{dist}(g_m(\mathbf{x}), g_m(\hat{\mathbf{x}}), id(\cdot)), \quad (7)$$

in which id denotes the identity function, i.e. $id(x) = x$.

Matching pair-wise features. Moreover, to further address the unique nature of the ISR task, which aims to reconstruct content with high fidelity and fine local details, we also introduce a pair-wise loss, \mathcal{L}_{pair} , within each local feature group described above. Specifically, for each synthetic feature patch assigned to a group, we identify the most similar real local feature patch within the same group and construct a pair. We then compute the L1 loss between the paired features to minimize their discrepancy. This is expected to encourage the synthetic data to better match the real data at the local detail level and to improve the fidelity of fine details and the overall visual quality of the synthesized images. This process can be described by the equation below:

$$\mathcal{L}_{pair} = \sum_{m=1}^M \sum_{i=1}^{N_m} \frac{1}{N_m} \|f''(\mathbf{x})^{g_m(i)} - f''(\hat{\mathbf{x}})^{g_m(i)}\|_1, \quad (8)$$

in which N_m is the number of feature patch pairs in the group m . $f''(\mathbf{x})^{g_m(i)}$ represents the real feature in the i^{th} pair, and $f''(\hat{\mathbf{x}})^{g_m(i)}$ is the corresponding synthetic feature in this pair.

These three losses are used at different stages in the proposed IDC framework for synthetic data optimization, and the training algorithm is described in Algorithm 1.

4 Experiment Configuration

Implementation details. IDC is a novel dataset condensation method specifically designed for the ISR task, which can be applied to any dataset with or without labels. In this experiment, we employ SwinIR [28] and MambaIRv2 [17] that are optimized on the original real training dataset \mathcal{T} obtained from DIV2K as the feature extractor and the up-sampling ISR model, respectively. For each instance/class, we can generate the synthetic dataset with a 10% condense ratio for 20k iterations with a single Nvidia-A40 GPU. For HR patch up-sampling, we choose one of the latest ISR models, MambaIRv2, due to its superior performance (test results are provided in *Supplementary*). Other detailed training and hyper-parameter configurations are also provided in *Supplementary*.

Datasets and metrics. To evaluate the performance of the proposed method, we used the widely used training dataset for ISR, DIV2K [1], as the original training dataset; this contains 800 images with a 2K resolution. We follow the common practice [48, 29, 60, 51, 28, 40, 43] to crop all the images into overlapped patches with a spatial resolution of 256×256 and down-sample them into corresponding LR patches (64×64) targeting the $\times 4$ task. This results in a total number of 120,765 HR-LR patch pairs, forming the real dataset \mathcal{T} mentioned above. For performance evaluation, we use five commonly used datasets [2, 58, 20, 34, 15] and perform the $\times 4$ ISR task. The performance has been measured by PSNR and SSIM [50].

Benchmarks. We compared the proposed methods with four dataset core-selection/pruning methods, including random selection, Herding [52], Kcenter [41] and DCSR [9]. All these benchmarks were applied on \mathcal{T} with the same ratio (10%) to obtain the selected/pruned (real) patches. We also provide the results based on the whole original training set \mathcal{T} for reference. We did not compare IDC to the only available dataset condensation method designed for ISR, GSDD [59], because it is only suitable for datasets with classification labels and was evaluated with GAN-based ISR models, which is not the common practice in ISR literature. Moreover, we did not directly benchmark our approach

Table 1: Comparison with coreset selection and dataset pruning methods. For all methods (except the Whole), we generated/selected 12,076 LR-HR pairs with the condense ratio $r=10\%$. The results are based on PSNR (dB) and SSIM. The best and second best results are highlighted in red and yellow cells, respectively.

PSNR (dB) \uparrow	Set5 [2]			Set14 [58]			Urban100 [20]		
	EDSR	SwinIR	MambaIRv2	EDSR	SwinIR	MambaIRv2	EDSR	SwinIR	MambaIRv2
Whole	30.17	30.28	30.52	26.61	26.78	26.88	24.50	24.92	25.21
Random	30.13	30.20	30.49	26.54	26.68	26.86	24.40	24.70	25.02
Herding [52]	29.94	30.03	30.36	26.43	26.54	26.65	24.10	24.40	24.65
Kcenter [41]	30.01	30.12	30.45	26.50	26.61	26.79	24.28	24.56	24.86
DCSR [9]	30.16	30.33	30.51	26.54	26.69	26.86	24.43	24.78	25.10
IDC (ours)	30.18	30.34	30.52	26.63	26.78	26.91	24.47	24.86	25.16

PSNR (dB) \uparrow	BSD100 [34]			Manga109 [15]		
	EDSR	SwinIR	MambaIRv2	EDSR	SwinIR	MambaIRv2
Whole	26.24	26.34	26.40	28.50	28.98	29.22
Random	26.19	26.28	26.37	28.32	28.74	29.07
Herding [52]	26.11	26.19	26.30	27.88	28.30	28.54
Kcenter [41]	26.17	26.25	26.34	28.19	28.64	28.89
DCSR [9]	26.21	26.31	26.39	28.42	28.86	29.14
IDC (ours)	26.24	26.34	26.40	28.54	29.02	29.26

SSIM \uparrow	Set5 [2]			Set14 [58]			Urban100 [20]		
	EDSR	SwinIR	MambaIRv2	EDSR	SwinIR	MambaIRv2	EDSR	SwinIR	MambaIRv2
Whole	0.8645	0.8679	0.8699	0.7435	0.7492	0.7507	0.7627	0.7769	0.7861
Random	0.8639	0.8664	0.8694	0.7424	0.7469	0.7498	0.7594	0.7707	0.7801
Herding [52]	0.8607	0.8646	0.8674	0.7397	0.7439	0.7455	0.7504	0.7617	0.7701
Kcenter [41]	0.8626	0.8655	0.8686	0.7412	0.7452	0.7481	0.7558	0.7674	0.7759
DCSR [9]	0.8642	0.8679	0.8696	0.7426	0.7478	0.7504	0.7608	0.7737	0.7825
IDC (ours)	0.8644	0.8680	0.8702	0.7445	0.7487	0.7516	0.7610	0.7749	0.7824

SSIM \uparrow	BSD100 [34]			Manga109 [15]		
	EDSR	SwinIR	MambaIRv2	EDSR	SwinIR	MambaIRv2
Whole	0.7137	0.7185	0.7202	0.8788	0.8877	0.8903
Random	0.7126	0.7172	0.7195	0.8767	0.8854	0.8889
Herding [52]	0.7102	0.7145	0.7174	0.8704	0.8792	0.8822
Kcenter [41]	0.7130	0.7162	0.7185	0.8776	0.8839	0.8860
DCSR [9]	0.7125	0.7178	0.7202	0.8773	0.8866	0.8895
IDC (ours)	0.7137	0.7184	0.7198	0.8795	0.8882	0.8895

against dataset condensation methods proposed for high-level vision tasks due to their label-based nature. However, we will do take them into account in the ablation study described below.

ISR models. Three popular ISR models including EDSR-baseline [29], SwinIR [28] and MambaIRv2 [17] have been trained here on different datasets generated by the proposed and benchmark methods in this experiment based on the same training configurations. The implementation details for other methods and training configurations are summarized in *Supplementary*.

5 Results and Discussion

Overall performance. Table 1 summarizes the comparison results between our proposed Instance Data Condensation (IDC) approach and other dataset selection and pruning methods for ISR. It can be observed that IDC consistently achieves superior performance compared to the benchmark methods, across most of the test datasets and quality metrics. In particular, with only 10% of the data volume, it offers even better evaluation performance compared to the whole original training set on four out of five datasets. We also provide visual examples of synthetic training patches in Figure 3, which show that IDC can preserve high-frequency details and texture information. As far as we are aware, this is the first data condensation method which achieves this level of performance for the ISR task.

Alongside evaluation performance, training datasets should also support reduced optimization time and stable training behavior. To assess these characteristics, we plot the performance comparison between our proposed IDC method, Random selection, and the DCSR approach on the Set14 dataset with different learning rates during the training process, using SwinIR as the ISR model with a 1% condensation ratio (a more challenging case). It has been observed that the DCSR method, which employs Sobel filters to preserve real high-gradient image regions, exhibits evident overfitting

Table 2: Results of the ablation study. \checkmark : included, \times : excluded. Here, we only condense 80 images/classes for each setting but with the same condense ratio 10% in each class (effectively 1% condense ratio for the whole dataset). We choose the EDSR-baseline [29] as the ISR model, evaluated on three test datasets.

Variant	Local Feature	Unfolding	Instance Loss	Group Loss	Pair Loss	Set5		Urban100		Manga109	
						PSNR	SSIM	PSNR	SSIM	PSNR	SSIM
IDC	\checkmark	\checkmark	\checkmark	\checkmark	\checkmark	30.02	0.8616	24.07	0.7474	28.00	0.8723
v1	\times	\times	\checkmark	\times	\times	-21.71	-0.7606	-16.60	-0.6674	-20.44	-0.7499
v2	\checkmark	\times	\checkmark	\times	\times	-0.49	-0.0092	-0.60	-0.0247	-0.56	-0.0108
v3	\checkmark	\checkmark	\checkmark	\times	\times	-0.16	-0.0024	-0.12	-0.0059	-0.04	-0.0015
v4	\checkmark	\checkmark	\checkmark	\checkmark	\times	-0.05	-0.0008	-0.04	-0.0020	0.06	0.0007
v5	\times	\checkmark	\checkmark	\checkmark	\checkmark	-0.19	-0.0023	-0.04	-0.0017	-0.06	-0.0005
v6	\checkmark	\times	\checkmark	\checkmark	\checkmark	-0.29	-0.0034	-0.10	-0.0048	-0.10	-0.0017
v7	\checkmark	\checkmark	\times	\checkmark	\checkmark	-0.22	-0.0032	-0.02	-0.0012	-0.09	-0.0011

behavior across all four different learning rate configurations. In contrast, our method demonstrates better stability and generalization capability, maintaining a steady upward trend throughout the training process.

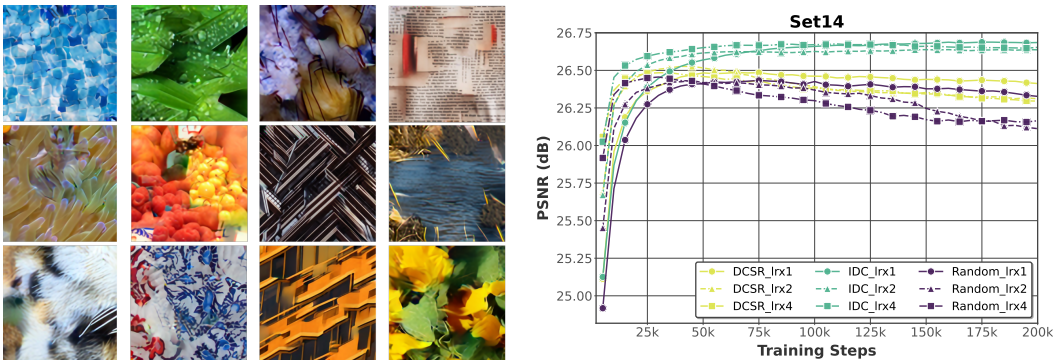


Figure 3: (Left): Visual Examples of our synthetic images. (Right): Validation trajectory on the Set14.



Figure 4: Starting from the original NCFD [46] (v1), the visual evolution for adding each contribution.

Ablation study. In order to compare our approach with SOTA dataset condensation methods proposed for high-level vision tasks, we first start with the original NCFD [46], and progressively add each component, resulting in four variants v1-v4. In addition, to thoroughly verify the contributions of the main components in the proposed IDC framework, we further obtained another three variants v5-v7 by removing Unfolding, Local Feature, Instance Loss, Group/Pair Losses (v3 already exists)¹, or Pair Loss (v4 already exists), respectively. The ablation results, based on Set5, Urban100 and Manga109 datasets, are shown in Table 2, which confirms the effectiveness and necessity of each component in the IDC framework. We also provide their synthetic patch examples of v1-v4 in Figure 4 for visualization. More details about the ablation experiments for the hyper-parameters setting will be provided in the *Supplementary*.

6 Conclusion

This paper presents Instance Data Condensation (IDC) specifically targeting image super-resolution tasks. It synthesizes a small yet informative training dataset from a large dataset containing real images. By leveraging a multi-level distribution matching framework and the new random local

¹We cannot solely remove Group loss as the Pair loss is based on the Group loss in our method.

Fourier features, IDC captures essential structural and textural features from the original high-resolution images and achieves significant data condensation. Trained on the resulting small synthetic dataset (with only 10% of the original data volume) ISR models can achieve comparable or (in some cases) even better performance compared to using the entire real training dataset (DIV2K), when benchmarked on multiple test datasets. As far as we are aware, this is the first data condensation approach designed for specifically ISR, capable of this level of performance. More importantly, compared to other benchmarks based on data selection and pruning, it offers better training stability and (potentially) improved data privacy. We recommend that future work should focus on further performance improvement and speeding up the condensation process.

References

- [1] E. Agustsson and R. Timofte. NTIRE 2017 challenge on single image super-resolution: Dataset and study. In *Proceedings of the IEEE conference on computer vision and pattern recognition workshops*, pages 126–135, 2017.
- [2] M. Bevilacqua, A. Roumy, C. Guillemot, and M.-L. A. Morel. Low-complexity single-image super-resolution based on nonnegative neighbor embedding. In *British Machine Vision Conference (BMVC)*, 2012.
- [3] G. Cazenavette, T. Wang, A. Torralba, A. A. Efros, and J.-Y. Zhu. Dataset distillation by matching training trajectories. In *Proceedings of the IEEE/CVF Conference on Computer Vision and Pattern Recognition*, pages 4750–4759, 2022.
- [4] D. Chen, R. Kerkouche, and M. Fritz. Private set generation with discriminative information. *Advances in Neural Information Processing Systems*, 35:14678–14690, 2022.
- [5] X. Chen, X. Wang, J. Zhou, Y. Qiao, and C. Dong. Activating more pixels in image super-resolution transformer. In *Proceedings of the IEEE/CVF Conference on Computer Vision and Pattern Recognition (CVPR)*, pages 22367–22377, June 2023.
- [6] J. Cui, R. Wang, S. Si, and C.-J. Hsieh. Scaling up dataset distillation to imagenet-1k with constant memory. In *International Conference on Machine Learning*, pages 6565–6590. PMLR, 2023.
- [7] W. Deng, W. Li, T. Ding, L. Wang, H. Zhang, K. Huang, J. Huo, and Y. Gao. Exploiting inter-sample and inter-feature relations in dataset distillation. In *Proceedings of the IEEE/CVF Conference on Computer Vision and Pattern Recognition*, pages 17057–17066, 2024.
- [8] T. Dietz, B. B. Moser, T. Nauen, F. Raue, S. Frolov, and A. Dengel. A study in dataset distillation for image super-resolution. *arXiv preprint arXiv:2502.03656*, 2025.
- [9] Q. Ding, Z. Liang, L. Wang, Y. Wang, and J. Yang. Not all patches are equal: Hierarchical dataset condensation for single image super-resolution. *IEEE Signal Processing Letters*, 30:1752–1756, 2023.
- [10] C. Dong, C. C. Loy, K. He, and X. Tang. Image super-resolution using deep convolutional networks. *IEEE transactions on pattern analysis and machine intelligence*, 38(2):295–307, 2015.
- [11] T. Dong, B. Zhao, and L. Lyu. Privacy for free: How does dataset condensation help privacy? In *International Conference on Machine Learning*, pages 5378–5396. PMLR, 2022.
- [12] J. Du, J. Hu, W. Huang, J. T. Zhou, et al. Diversity-driven synthesis: Enhancing dataset distillation through directed weight adjustment. *Advances in neural information processing systems*, 37:119443–119465, 2024.
- [13] J. Du, Y. Jiang, V. Y. Tan, J. T. Zhou, and H. Li. Minimizing the accumulated trajectory error to improve dataset distillation. In *Proceedings of the IEEE/CVF conference on computer vision and pattern recognition*, pages 3749–3758, 2023.
- [14] C. Finn, P. Abbeel, and S. Levine. Model-agnostic meta-learning for fast adaptation of deep networks. In *International conference on machine learning*, pages 1126–1135. PMLR, 2017.
- [15] A. Fujimoto, T. Ogawa, K. Yamamoto, Y. Matsui, T. Yamasaki, and K. Aizawa. Manga109 dataset and creation of metadata. In *Proceedings of the 1st international workshop on comics analysis, processing and understanding*, pages 1–5, 2016.
- [16] D. Ganguli, D. Hernandez, L. Lovitt, A. Askell, Y. Bai, A. Chen, T. Conerly, N. Dassarma, D. Drain, N. Elhage, et al. Predictability and surprise in large generative models. In *Proceedings of the 2022 ACM Conference on Fairness, Accountability, and Transparency*, pages 1747–1764, 2022.
- [17] H. Guo, Y. Guo, Y. Zha, Y. Zhang, W. Li, T. Dai, S.-T. Xia, and Y. Li. MambaIRv2: Attentive state space restoration. *arXiv preprint arXiv:2411.15269*, 2024.
- [18] H. Guo, J. Li, T. Dai, Z. Ouyang, X. Ren, and S.-T. Xia. MambaIR: A simple baseline for image restoration with state-space model. In *ECCV*, 2024.

- [19] G. Hinton, O. Vinyals, and J. Dean. Distilling the knowledge in a neural network. *arXiv preprint arXiv:1503.02531*, 2015.
- [20] J.-B. Huang, A. Singh, and N. Ahuja. Single image super-resolution from transformed self-exemplars. In *Proceedings of the IEEE conference on computer vision and pattern recognition*, pages 5197–5206, 2015.
- [21] Y. Jiang, H. M. Kwan, T. Peng, G. Gao, F. Zhang, X. Zhu, J. Sole, and D. Bull. HIIF: Hierarchical encoding based implicit image function for continuous super-resolution. *arXiv preprint arXiv:2412.03748*, 2024.
- [22] Y. Jiang, C. Zeng, S. Teng, F. Zhang, X. Zhu, J. Sole, and D. Bull. C2D-ISR: Optimizing attention-based image super-resolution from continuous to discrete scales. *arXiv preprint arXiv:2503.13740*, 2025.
- [23] A. Katharopoulos and F. Fleuret. Not all samples are created equal: Deep learning with importance sampling. In *International conference on machine learning*, pages 2525–2534. PMLR, 2018.
- [24] J. Kim, J. K. Lee, and K. M. Lee. Accurate image super-resolution using very deep convolutional networks. In *Proceedings of the IEEE conference on computer vision and pattern recognition*, pages 1646–1654, 2016.
- [25] H. Li, Y. Zhou, X. Gu, B. Li, and W. Wang. Diversified semantic distribution matching for dataset distillation. In *Proceedings of the 32nd ACM International Conference on Multimedia*, pages 7542–7550, 2024.
- [26] Y. Li, K. Zhang, J. Liang, J. Cao, C. Liu, R. Gong, Y. Zhang, H. Tang, Y. Liu, D. Demandolx, et al. LSDIR: A large scale dataset for image restoration. In *Proceedings of the IEEE/CVF Conference on Computer Vision and Pattern Recognition*, pages 1775–1787, 2023.
- [27] J. Liang, J. Cao, Y. Fan, K. Zhang, R. Ranjan, Y. Li, R. Timofte, and L. Van Gool. VRT: A video restoration transformer. *arXiv preprint arXiv:2201.12288*, 2022.
- [28] J. Liang, J. Cao, G. Sun, K. Zhang, L. Van Gool, and R. Timofte. SwinIR: Image restoration using swin transformer. In *Proceedings of the IEEE/CVF international conference on computer vision*, pages 1833–1844, 2021.
- [29] B. Lim, S. Son, H. Kim, S. Nah, and K. Mu Lee. Enhanced deep residual networks for single image super-resolution. In *Proceedings of the IEEE conference on computer vision and pattern recognition workshops*, pages 136–144, 2017.
- [30] Z. Lin, P. Garg, A. Banerjee, S. A. Magid, D. Sun, Y. Zhang, L. Van Gool, D. Wei, and H. Pfister. Revisiting RCAN: Improved training for image super-resolution. *arXiv preprint arXiv:2201.11279*, 2022.
- [31] Y. Liu, A. Liu, J. Gu, Z. Zhang, W. Wu, Y. Qiao, and C. Dong. Discovering distinctive "semantics" in super-resolution networks. *arXiv preprint arXiv:2108.00406*, 2021.
- [32] L. Lyu, H. Yu, and Q. Yang. Threats to federated learning: A survey. *arXiv preprint arXiv:2003.02133*, 2020.
- [33] D. Maclaurin, D. Duvenaud, and R. Adams. Gradient-based hyperparameter optimization through reversible learning. In *International conference on machine learning*, pages 2113–2122. PMLR, 2015.
- [34] D. Martin, C. Fowlkes, D. Tal, and J. Malik. A database of human segmented natural images and its application to evaluating segmentation algorithms and measuring ecological statistics. In *Proceedings eighth IEEE international conference on computer vision. ICCV 2001*, volume 2, pages 416–423. IEEE, 2001.
- [35] L. Melis, C. Song, E. De Cristofaro, and V. Shmatikov. Exploiting unintended feature leakage in collaborative learning. In *2019 IEEE symposium on security and privacy (SP)*, pages 691–706. IEEE, 2019.
- [36] B. B. Moser, F. Raue, and A. Dengel. A study in dataset pruning for image super-resolution. In *International Conference on Artificial Neural Networks*, pages 351–363. Springer, 2024.
- [37] G. Ohtani, R. Tadokoro, R. Yamada, Y. M. Asano, I. Laina, C. Rupprecht, N. Inoue, R. Yokota, H. Kataoka, and Y. Aoki. Rethinking image super-resolution from training data perspectives. In *European Conference on Computer Vision*, pages 19–36. Springer, 2024.
- [38] M. Paul, S. Ganguli, and G. K. Dziugaite. Deep learning on a data diet: Finding important examples early in training. *Advances in neural information processing systems*, 34:20596–20607, 2021.
- [39] J. M. Phillips. Coresets and sketches. In *Handbook of discrete and computational geometry*, pages 1269–1288. Chapman and Hall/CRC, 2017.
- [40] Y. Ren, X. Li, M. Guo, B. Li, S. Zhao, and Z. Chen. MambaCSR: Dual-interleaved scanning for compressed image super-resolution with ssms, 2024.
- [41] O. Sener and S. Savarese. Active learning for convolutional neural networks: A core-set approach. *ICLR*, 2018.
- [42] S. Shao, Z. Yin, M. Zhou, X. Zhang, and Z. Shen. Generalized large-scale data condensation via various backbone and statistical matching. In *Proceedings of the IEEE/CVF Conference on Computer Vision and Pattern Recognition*, pages 16709–16718, 2024.

- [43] Y. Shi, B. Xia, X. Jin, X. Wang, T. Zhao, X. Xia, X. Xiao, and W. Yang. VmambaIR: Visual state space model for image restoration. *IEEE Transactions on Circuits and Systems for Video Technology*, 2025.
- [44] R. Timofte, E. Agustsson, L. Van Gool, M.-H. Yang, and L. Zhang. NTIRE 2017 challenge on single image super-resolution: Methods and results. In *Proceedings of the IEEE conference on computer vision and pattern recognition workshops*, pages 114–125, 2017.
- [45] K. Wang, B. Zhao, X. Peng, Z. Zhu, S. Yang, S. Wang, G. Huang, H. Bilen, X. Wang, and Y. You. CAfE: Learning to condense dataset by aligning features. In *Proceedings of the IEEE/CVF Conference on Computer Vision and Pattern Recognition*, pages 12196–12205, 2022.
- [46] S. Wang, Y. Yang, Z. Liu, C. Sun, X. Hu, C. He, and L. Zhang. Dataset distillation with neural characteristic function: A minmax perspective. *arXiv preprint arXiv:2502.20653*, 2025.
- [47] T. Wang, J.-Y. Zhu, A. Torralba, and A. A. Efros. Dataset distillation. *arXiv preprint arXiv:1811.10959*, 2018.
- [48] X. Wang, L. Xie, K. Yu, K. C. Chan, C. C. Loy, and C. Dong. BasicSR: Open source image and video restoration toolbox. <https://github.com/XPiXeIGroup/BasicSR>, 2022.
- [49] X. Wang, K. Yu, C. Dong, and C. C. Loy. Recovering realistic texture in image super-resolution by deep spatial feature transform. In *Proceedings of the IEEE conference on computer vision and pattern recognition*, pages 606–615, 2018.
- [50] Z. Wang, A. C. Bovik, H. R. Sheikh, and E. P. Simoncelli. Image quality assessment: from error visibility to structural similarity. *IEEE transactions on image processing*, 13(4):600–612, 2004.
- [51] Z. Wang, X. Cun, J. Bao, W. Zhou, J. Liu, and H. Li. Uformer: A general U-shaped transformer for image restoration. In *Proceedings of the IEEE/CVF conference on computer vision and pattern recognition*, pages 17683–17693, 2022.
- [52] M. Welling. Herding dynamical weights to learn. In *Proceedings of the 26th annual international conference on machine learning*, pages 1121–1128, 2009.
- [53] J. Yang, J. Wright, T. S. Huang, and Y. Ma. Image super-resolution via sparse representation. *IEEE transactions on image processing*, 19(11):2861–2873, 2010.
- [54] Q. Yang, D. Chen, Z. Tan, Q. Liu, Q. Chu, J. Bao, L. Yuan, G. Hua, and N. Yu. HQ-50K: A large-scale, high-quality dataset for image restoration. *arXiv preprint arXiv:2306.05390*, 2023.
- [55] Z. Yin, E. Xing, and Z. Shen. Squeeze, recover and relabel: Dataset condensation at imagenet scale from a new perspective. *Advances in Neural Information Processing Systems*, 36:73582–73603, 2023.
- [56] R. Yu, S. Liu, and X. Wang. Dataset distillation: A comprehensive review. *IEEE transactions on pattern analysis and machine intelligence*, 46(1):150–170, 2023.
- [57] R. Yu, S. Liu, J. Ye, and X. Wang. Teddy: Efficient large-scale dataset distillation via taylor-approximated matching. In *European Conference on Computer Vision*, pages 1–17. Springer, 2024.
- [58] R. Zeyde, M. Elad, and M. Protter. On single image scale-up using sparse-representations. In *Curves and Surfaces: 7th International Conference, Avignon, France, June 24-30, 2010, Revised Selected Papers 7*, pages 711–730. Springer, 2012.
- [59] H. Zhang, S. Su, Y. Zhu, J. Sun, and Y. Zhang. GSDD: Generative space dataset distillation for image super-resolution. In *Proceedings of the AAI Conference on Artificial Intelligence*, volume 38 (07), pages 7069–7077, 2024.
- [60] Y. Zhang, K. Li, K. Li, L. Wang, B. Zhong, and Y. Fu. Image super-resolution using very deep residual channel attention networks. In *Proceedings of the European conference on computer vision (ECCV)*, pages 286–301, 2018.
- [61] B. Zhao and H. Bilen. Dataset condensation with distribution matching. In *Proceedings of the IEEE/CVF Winter Conference on Applications of Computer Vision*, pages 6514–6523, 2023.
- [62] B. Zhao, K. R. Mopuri, and H. Bilen. Dataset condensation with gradient matching. In *Ninth International Conference on Learning Representations 2021*, 2021.
- [63] G. Zhao, G. Li, Y. Qin, and Y. Yu. Improved distribution matching for dataset condensation. In *Proceedings of the IEEE/CVF Conference on Computer Vision and Pattern Recognition*, pages 7856–7865, 2023.
- [64] Y. Zhou, Z. Li, C.-L. Guo, S. Bai, M.-M. Cheng, and Q. Hou. SRFormer: Permuted self-attention for single image super-resolution. In *Proceedings of the IEEE/CVF International Conference on Computer Vision*, pages 12780–12791, 2023.
- [65] Y. Zhou, E. Nezhadarya, and J. Ba. Dataset distillation using neural feature regression. *Advances in Neural Information Processing Systems*, 35:9813–9827, 2022.